AIP | Journal of Applied Physics

Depth dependence of ultraviolet curing of organosilicate low-k thin films

Taek-Soo Kim, Naoto Tsuji, Nathan Kemeling, Kiyohiro Matsushita, Dmytro Chumakov et al.

Citation: J. Appl. Phys. 103, 064108 (2008); doi: 10.1063/1.2894727
View online: http://dx.doi.org/10.1063/1.2894727
View Table of Contents: http://jap.aip.org/resource/1/JAPIAU/v103/i6
Published by the American Institute of Physics.

Additional information on J. Appl. Phys.

Journal Homepage: http://jap.aip.org/
Journal Information: http://jap.aip.org/about/about_the_journal
Top downloads: http://jap.aip.org/features/most_downloaded
Information for Authors: http://jap.aip.org/authors

ADVERTISEMENT

Downloaded 21 Apr 2013 to 143.248.118.125. This article is copyrighted as indicated in the abstract. Reuse of AIP content is subject to the terms at: http://jap.aip.org/about/rights_and_permissions

JOURNAL OF APPLIED PHYSICS **103**, 064108 (2008)

Depth dependence of ultraviolet curing of organosilicate low-*k* thin films

Taek-Soo Kim,[1] Naoto Tsuji,[2] Nathan Kemeling,[2] Kiyohiro Matsushita,[2]
Dmytro Chumakov,[3] Holm Geisler,[3] Ehrenfried Zschech,[3] and Reinhold H. Dauskardt[4,a]
[1]*Department of Mechanical Engineering, Stanford University, Stanford, California 94305, USA*
[2]*ASM Japan K.K., 23-1, 6-chome Nagayama, Tama-shi, Tokyo, 206-0025, Japan*
[3]*AMD Saxony LLC & Co. KG, Wilschdorfer Landstrasse 101, Dresden, Saxony, D-01109, Germany*
[4]*Department of Materials Science and Engineering, Stanford University, Stanford, California 94305, USA*

(Received 17 October 2007; accepted 11 January 2008; published online 25 March 2008)

UV radiation curing has emerged as a promising postdeposition curing treatment to strengthen organosilicate interlayer dielectric thin films. We provide the evidence of film depth dependent UV curing which has important effects on through thickness mechanical and fracture properties. Force modulation atomic force microscopy measurements of the elastic modulus through the thickness of the films revealed evidence of periodic modulations of the glass stiffness which increased in magnitude with UV curing time. Furthermore, while significant increases in fracture energy were observed with UV curing time at the top of the organosilicate film, much lower increases were observed at the bottom. The increase in fracture energy with UV curing was film thickness dependent. The cohesive fracture resistance was less sensitive to UV curing. Possible explanations for the stiffness modulations through the film thickness involving UV light interference or phase separation by spinodal decomposition during the cure process are described. © *2008 American Institute of Physics*. [DOI: 10.1063/1.2894727]

INTRODUCTION

Organosilicate thin-film glasses are superior candidates for use as low dielectric constant interlayer dielectrics. However, their mechanically fragile nature and susceptibility to moisture assisted cracking have made integration into complex device structures challenging.[1–4] Significant efforts are being directed to improving their mechanical properties by manipulating the glass structure through the use of postdeposition curing treatments using external energy sources such as thermal, plasma,[5] e-beam,[6] and UV radiation.[7] UV curing, especially, has emerged as a promising method to strengthen the organosilicate glasses and has been demonstrated to significantly increase elastic modulus, hardness, and interfacial fracture energy while inducing relatively minor increases in dielectric constant and film density.[8–10] Selective molecular photolysis and specific photochemical reactions can be achieved by irradiation with an appropriate choice of the UV radiation energy spectrum.[8,11] UV curing results in the removal of certain nonbridging terminal bonds such as $Si-CH_3$ and Si–OH and a subsequent formation of cross-linked Si–O–Si bonds.[8,10,12,13] Detailed characterization by nuclear magnetic resonance spectroscopy and Fourier transform infrared spectroscopy showed significant changes in glass structure with increasing curing time, marked by the removal of terminal organic groups and increased network forming bonds following the initial removal of a porogen material.[10]

In the present study, we investigated in detail the role of UV curing time and dielectric film thickness on the mechanical and fracture properties of organosilicate thin films. We demonstrate that the higher degree of film connectivity brought about by increased UV cure duration significantly enhances the fracture energy at the top of the organosilicate layer while surprisingly has little effect on the fracture resistance at the bottom of the layer. Moreover, UV curing appeared to have little effect on the film cohesive fracture resistance in the middle of the layer except for the longest UV cure times. For a given UV cure, the fracture energy for all fracture locations through the film depth was found to decrease significantly as the organosilicate layer thickness was increased. On the other hand, the film stress and elastic modulus which represent bulk properties of the film increased in direct proportion to the UV curing time over the curing times examined.

A particularly surprising finding of the present study, however, was a direct evidence of film depth dependent UV curing that we recently reported in a preliminary study.[14] Force modulation-atomic force microscopy (FM-AFM) measurements of the elastic modulus through the thickness of the films revealed evidence of periodic modulations of the glass stiffness which increased in magnitude with UV curing time. While the film depth dependent curing may be related to a number of phenomena as discussed later, we believe the principal reason is associated with UV light interference which forms a standing wave during the curing process. The standing wave results in a nonuniform film depth dependent cure profile that is modified from the standing wave wavelength by shrinkage of the film during curing. The resulting nonuniform cure has important implications for resulting film mechanical and fracture properties.

EXPERIMENTAL DETAILS

A series of experimental organosilicate films with thicknesses of 400, 600, and 800 nm were deposited by plasma enhanced chemical vapor deposition (PECVD) onto silicon

[a]Electronic mail: dauskardt@stanford.edu.

 © 2008 American Institute of Physics

Downloaded 21 Apr 2013 to 143.248.118.125. This article is copyrighted as indicated in the abstract. Reuse of AIP content is subject to the terms at: http://jap.aip.org/about/rights_and_permissions

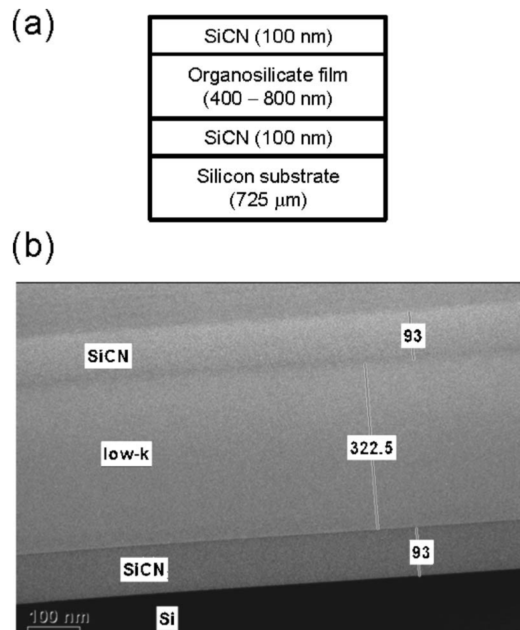

FIG. 1. (a) Schematic illustration of the thin film structure containing a PECVD organosilicate film and PECVD SiCN films. (b) The bright field TEM image of the film structure containing an UVx5 cured 400 nm organosilicate film. Film thicknesses are shown in the unit of nanometers.

wafers containing a 100 nm thick SiCN barrier layer [Fig. 1(a)]. The material did not include a porogen. After deposition of the organosilicate films, all the films were exposed to monochromatic UV radiation (wavelength <200 nm) for a selected duration in a controlled environment, which will be referred to as UVx1. 400 nm thick organosilicate films were UV cured for various durations ranging from one (UVx1) to five (UVx5) multiple cure times. We note that for the longer UV-cure times the UV-cure was continuous and not interrupted. Following the UV-cure, the organosilicate films were capped with a 100 nm thick SiCN layer without a predeposition plasma treatment. Focused ion beam (FIB) milling was used to prepare transmission electron microscopy (TEM) samples. Elastic moduli were measured by nanoindentation on the top surface of organosilicate films before they were capped and also on the cross-sections of the films in the specimens prepared for the FM-AFM measurements described below. The dielectric constant, index of refraction, elastic modulus, hardness, and film stress for the 400 nm organosilicate films are summarized in Table I. Film stress was measured using wafer curvature techniques. The film stresses shown in Table I are only for the organosilicate layers and separate from the film stresses of the SiCN layers.

The FM-AFM technique was used to investigate the variations in the elastic modulus on the cross-section of specimens containing UV cured 400 nm organosilicate films. Two thin film structures shown in Fig. 1(a) were bonded with epoxy, and the specimen consisting of the two thin film structures were diced and polished by chemical-mechanical planarization (CMP) to produce a flat cross-section. During the FM scans on the cross-section the AFM tip always remained in contact with the surface. The quantitative estimation of the elastic modulus is based on the modeling of the mechanics of the tip-specimen elastic interaction. The calculations rely on the well-understood and commonly accepted Hertz model.[15] This model considers the deformation of both the surface and the tip. Present FM-AFM measurements require the knowledge of the reduced modulus at any two locations on the sample that possesses different elastic modulus values. These values are needed for the calibration of tip and cantilever parameters that play a determinant role in delivering the quantitative information. The corresponding calibration was performed by using a nanoindentation tool with *in situ* SPM imaging capability on sample regions which are still large enough to be measured with the tip of the nanoindenter. Further details of the FM-AFM technique were reported elsewhere.[16,17]

Depth profiles for the elemental compositions of organosilicate thin films were made by high resolution x-ray photoelectron spectroscopy (XPS) (Surface Science Instruments, S-Probe, Mountain View, CA) using Ar ion etching. To make sure the analyses were performed in the flat center of the $2 \times 2\ \mathrm{mm}^2$ etch crater in a specimen, an x-ray spot size of $150 \times 800\ \mu\mathrm{m}^2$ was used for individual elemental scans.

Four-point bend (FPB) and double cantilever beam (DCB) specimen geometries were fabricated for fracture energy and crack growth testing by sandwiching the films between two elastic silicon substrates using previously reported epoxy bonding techniques.[18] The interface fracture energy near the top or bottom of the organosilicate films was measured using the FPB technique with inner and outer pin spacings of 27 and 40 mm, respectively, and a constant displacement rate of $0.5\ \mu\mathrm{m/s}$.[19] The fracture location was determined by notching in either side of the resulting FPB

TABLE I. Material properties including dielectric constant, index of refraction, elastic modulus, hardness, and residual film stress for the 400 nm organosilicate films UV-cured for various times. Standard deviations are indicated. Significant linear increases in elastic modulus and residual film stress in terms of UV curing time were observed.

Curing time t (a.u.)	Dielectric constant k	Index of refraction (IR)	Elastic modulus E (GPa)		Hardness H (GPa), Nanoindentation on the cross-section	Residual film stress σ_f (MPa)
			Nanoindentation on the top surface	Nanoindentation on the cross-section		
0	2.62	1.3597	5.5 ± 0.17	⋯	⋯	60
1	2.59	1.3605	6.9 ± 0.21	8.6 ± 0.3	1.23 ± 0.06	68.3
2	2.62	1.3665	9.3 ± 0.28	⋯	⋯	75.6
3	2.66	1.3725	11.3 ± 0.34	11.8 ± 0.3	1.54 ± 0.08	83.3
5	2.72	⋯	15.2 ± 0.46	⋯	⋯	101

Downloaded 21 Apr 2013 to 143.248.118.125. This article is copyrighted as indicated in the abstract. Reuse of AIP content is subject to the terms at: http://jap.aip.org/about/rights_and_permissions

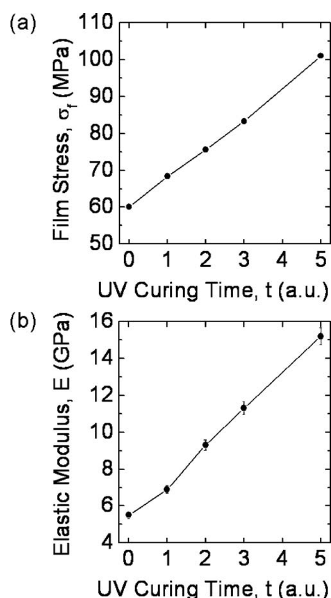

FIG. 2. (a) Residual film stress and (b) elastic modulus as a function of UV curing time.

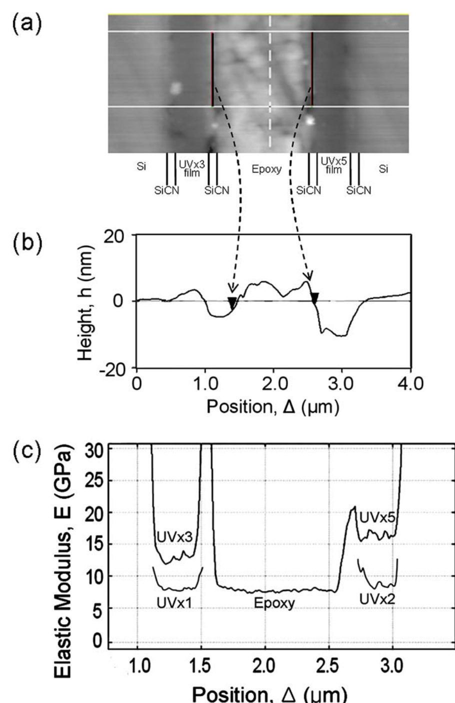

FIG. 3. (Color online) (a) The FM signal image of a cross-section of the (UVx3 cured 400 nm organosilicate film/epoxy/UVx5 cured 400 nm organosilicate film) specimen, (b) the topography plot in terms of the horizontal scanning position, and (c) elastic modulus as a function of scanning position.

specimen. The cohesive fracture energy was measured by the double cantilever beam technique.[20] Cracks were introduced in the organosilicate film using a prenotch in the DCB specimen and loading until fracture initiated. The DCB test configuration typically produces cohesive fracture in the center of the brittle organosilicate layer which was observed for all tests conducted. Crack growth rates da/dt were characterized as a function of the applied strain energy release rate G (J/m^2), over the range of $\sim 10^{-4} - \sim 10^{-10}$ m/s using load relaxation fracture mechanics techniques with the DCB specimens.[21] This involved loading the specimen at a constant displacement rate to a predetermined load then fixing the displacement. The following time-dependent load relaxation resulting from crack growth increases the specimen compliance from which the crack length a, da/dt, and G may be determined. Tests were conducted in an environmental chamber with temperature and humidity control of 30 ± 0.5 °C and $50 \pm 2\%$ relative humidity, respectively. After testing, the specimens were examined using XPS to determine the fracture path in the thin-film structures. A spot size of $150 \times 1000\ \mu m^2$ was used to perform survey scans for the binding energy range of 0–1000 eV.

RESULTS AND DISCUSSION

Significant film shrinkage was observed for all of the organosilicate films following UV curing. A representative bright field TEM image of the cross-section of an initially 400 nm thick organosilicate film following an UVx5 cure is shown in Fig. 1(b). The final film thickness was ~323 nm, representing ~19% shrinkage for the UVx5 cure. In the plane of the film, shrinkage is prevented because the film is attached to the underlying silicon substrate. As a result in-plane biaxial tensile stresses develop in the film. The resulting film stress as a function of UV curing time is shown in Fig. 2(a). The elastic modulus was also observed to increase with UV curing time and is shown for the initially 400 nm thick organosilicate films in Fig. 2(b). Although the elastic modulus values were obtained from nanoindentation with only limited penetration (~6%) into the film, the values were consistent with the FM-AFM elastic property values measured through the film thickness as described below.

A typical FM signal image of a cross-section of the specimen containing two organosilicate layers UV cured x3 and x5, respectively, is shown in Fig. 3(a). During the FM scans on the cross-section, the AFM tip always remained in contact with the surface exercising a pressure that strongly exceeds any variation in adhesive forces. A topography plot in terms of the horizontal scanning position is shown in Fig. 3(b). Although the topography of the low-k films showed some dishing, which is typical for CMP-polished specimens, such topography would not significantly affect the measurements of the elastic modulus.[16,17] The variation of the elastic modulus was measured through the 400 nm organosilicate film UV cured x1, x2, x3, and x5, and plotted as a function of the horizontal scanning position in Fig. 3(c). Careful observation of the modulus variation shown in Fig. 3(c) revealed clear and reproducible evidence of oscillations of the elastic modulus. The maximum amplitude of the modulus oscillation through the UV cured film is plotted as a function of cure time in Fig. 4. The amplitude of the oscillation became more pronounced with increasing UV cure duration. Although the amplitudes of the oscillating elastic modulus for the UVx1 cured films were in the maximum signal noise range estimated from the topography variation and the PID control of the AFM instrument, those for the UVx2, x3 and x5 clearly exceeded the signal noise levels. The effects of possible artifacts were minimal and the measurements

Downloaded 21 Apr 2013 to 143.248.118.125. This article is copyrighted as indicated in the abstract. Reuse of AIP content is subject to the terms at: http://jap.aip.org/about/rights_and_permissions

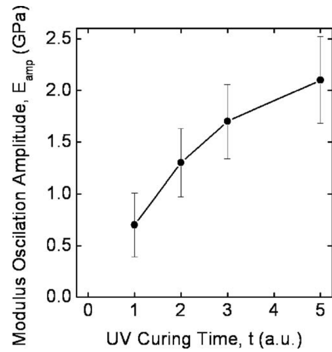

FIG. 4. The maximum amplitude of the modulus oscillation through the UV cured organosilicate film is plotted as a function of cure time.

proved to be repeatable in other locations and film cross sections. Note that a steep change of the topography and the large elastic modulus difference of the UVx5 film and the SiCN layer are believed to cause the lower elastic modulus of the SiCN layer as shown in Fig. 3(c). However, the dished topography of the low-*k* films would not cause any oscillationlike artifacts in the elastic modulus. The mean value of the elastic modulus through the film measured by FM-AFM was found to increase with increasing UV curing time, which is in good agreement with the nanoindenter measurement as shown in Table I.

The chemical composition of the organosilicate films and their dependence on film thickness and UV cure was investigated by XPS depth profiling (Fig. 5). Similar to previous studies[8–10,12,13] the carbon content was observed to decrease with UV curing indicative of the removal of nonbridging terminal bonds such as Si–CH_3 and a subsequent formation of cross-linked Si–O–Si bonds. In addition, we noted that the carbon content of the UVx1 cured organosilicate films decreased with decreasing film thickness, suggesting that the UV cure was less effective in reducing methyl groups and increasing the glass network bonds for the thicker films. Close inspection of the XPS profiles revealed no apparent evidence of a compositional variation of any of the observed elements that might correspond to the oscillation in elastic modulus. However, the XPS depth profiling technique is not likely to reveal subtle compositional variations. Accordingly, further studies using electron-energy-loss spectroscopy (EELS) composition profile taken in scanning transmission electron microscopy (STEM) mode and secondary ion-mass spectroscopy (SIMS) analysis through the film depth also did not reveal any evidence of compositional variations.[22] Taken together, these results imply that even subtle changes in the elemental composition below the detection limit of the above techniques following UV curing may result in periodic changes in the glass structure which has a substantial and measurable effect on the resulting glass elastic stiffness.

The role of organosilicate film thickness during UV curing on the fracture energy near the top and bottom of the organosilicate films is shown in Fig. 6. The interface fracture energy increased significantly by ~45% at the top interface and ~20% at the bottom interface for the initially 400 nm thick organosilicate film after UVx1 curing. However,

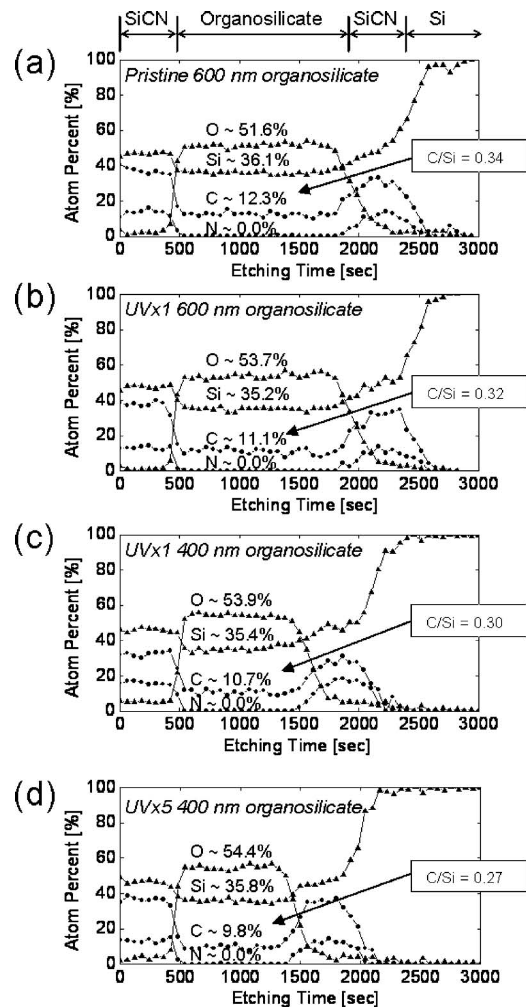

FIG. 5. XPS depth profiles for (a) pristine 600 nm, (b) UVx1 cured 600 nm, (c) UVx1 cured 400 nm, and (d) UVx5 cured 400 nm organosilicate film specimens. Relative atom percents of oxygen (closed triangle), silicon (open triangle), carbon (closed circle), and nitrogen (open circle) were analyzed. Note that XPS cannot detect hydrogen, which is a major element of organosilicate films.

thicker organosilicate films exhibited smaller increases in fracture energy after UVx1 curing. The decreased effect of the UV cure at the top interface of the thicker films was particularly unexpected because the top surfaces of all organosilicate films were exposed to the same UV radiation during curing. UV absorption occurs through the thickness of the organosilicate film and may be used to rationalize the decreased effects of UV cure towards the bottom of the layer. However, the top of the film presumably is exposed to the radiation before any absorption. The reason for the significant decrease in fracture energy towards the top of the layer may be related to UV standing wave effects as described later in this paper.

The effects of UV curing time on the fracture energy near the top and bottom interfaces, together with cohesive fracture energy measured in the middle of organosilicate films are shown in Fig. 7. While the fracture energies at the top interface increased significantly by ~422% with UVx5 curing, the fracture energy at the bottom interface exhibited little change, increasing by ~12%. The cohesive fracture

Downloaded 21 Apr 2013 to 143.248.118.125. This article is copyrighted as indicated in the abstract. Reuse of AIP content is subject to the terms at: http://jap.aip.org/about/rights_and_permissions

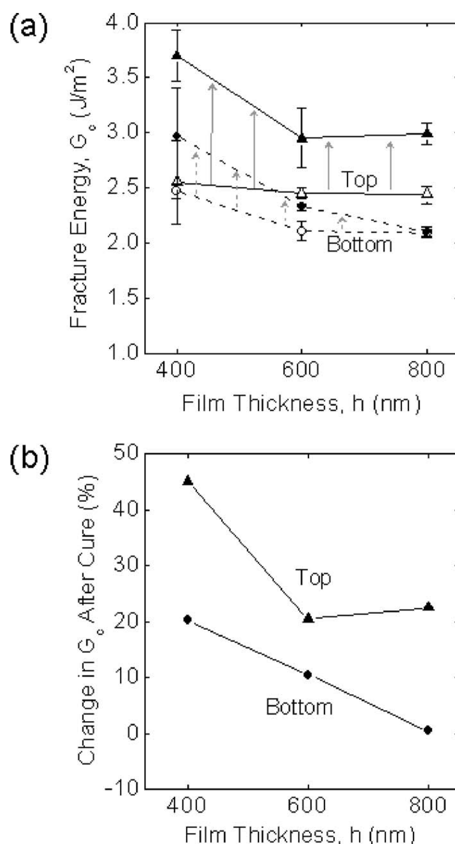

FIG. 6. (a) Fracture energies Gc at the top interfaces of as-deposited (open triangle) and UVx1 cured (closed triangle) organosilicate films are compared with those at the bottom interfaces of as-deposited (open circle) and UVx1 cured (closed circle) organosilicate films in terms of the film thickness. (b) Percent change in Gc after UVx1 curing at the top interfaces (triangle) and the bottom interfaces (circle) of organosilicate films.

energy of $\sim 2.4\ \mathrm{J/m^2}$ exhibited no observable change for curing to UVx3, following which a marginal increase of 12% was observed.

The effects of UV cure on the moisture-assisted crack growth rates in the initially 400 nm thick organosilicate films as a function of applied G measured in a 50% RH moist air environment are shown in Fig. 8. Similar to the cohesive fracture energy, there was no observable effect of curing up to UVx3 on the crack growth rate curves. Similar to our

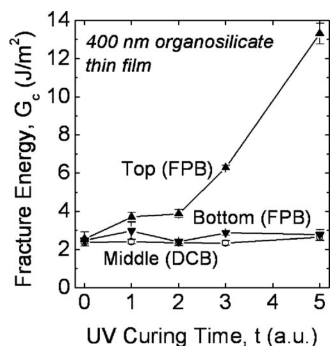

FIG. 7. Fracture energy of 400 nm organosilicate films as a function of multiple UV cure times. Fracture energies at top (up triangle) and bottom (down triangle) interfaces of organosilicate films were measured by FPB tests, and DCB tests were used for the cohesive fracture energies in the middle of organosilicate films (open circle) in the laboratory air.

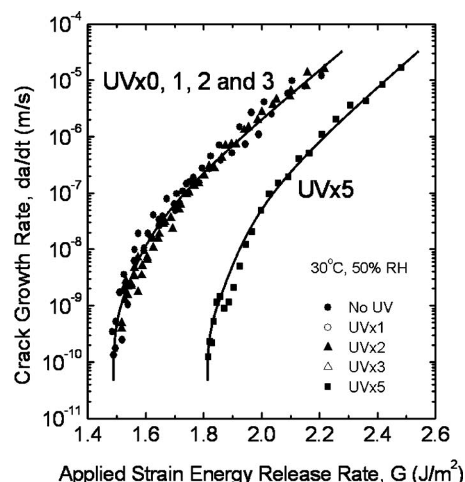

FIG. 8. Environmentally assisted cracking of 400 nm organosilicate films UV cured with various curing times were measured by DCB. All tests were performed in the environmental chamber at the constant temperature of 30 °C and relative humidity of 50%.

previous observations,[10,12] we believe that this is associated with the ability of the cohesive crack to meander through the glass network along weak microstructural paths through the glass network. As the glass network connectivity is initially increased by UV curing, the crack simply moves to other regions of the network that offer low network connectivity, thus reducing the effect of the cure on fracture resistance. Only after curing to UVx5 a significant increase in fracture resistance was observed. These results are interesting in that they highlight the significant effect that UV curing and network connectivity have on "bulk" film properties such as the elastic modulus and film stress that increase significantly and fracture properties that may be rather insensitive because the unconstrained cohesive crack path can bypass the initial increase in network bonds. The constrained fracture path on the top of the layer is forced to intercept all newly formed network bonds and hence exhibits a marked sensitivity to UV cure.

We now consider possible mechanisms that might account for the depth dependent modulus variation observed. The most likely initial mechanism to consider is phase separation by spinodal decomposition of the glass. Glasses are well known to undergo various spinodal decomposition processes leading to compositional variation and interpenetrating glass networks.[23] Further, it has been shown that UV irradiation in glass can lead to chemical migration either because of an increase of atom mobility or because the gradient of UV light introduces a new thermal driving force for diffusion.[24,25] Spinodal decomposition is characterized by a continuous variation of composition with time until equilibrium compositions are reached as shown schematically in Fig. 9.[26] The interface between phases is initially very diffuse and eventually sharpens given sufficient time and temperature.[26–28] In the case of our thin film glasses, the decomposition may occur through the thickness of the film as plane waves of compositional variation. This form of spinodal decomposition has, in fact, been observed in polymer thin films.[29] As noted above, no evidence for the compositional variation was observed in the present study. It is pos-

Downloaded 21 Apr 2013 to 143.248.118.125. This article is copyrighted as indicated in the abstract. Reuse of AIP content is subject to the terms at: http://jap.aip.org/about/rights_and_permissions

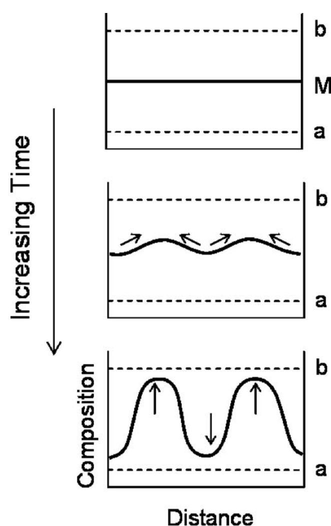

FIG. 9. Spinodal decomposition as a function of time. A small fluctuation in composition gradually grows over a period time via uphill diffusion. "*a*" and "*b*" are the final (limiting) compositions of the separate phases.

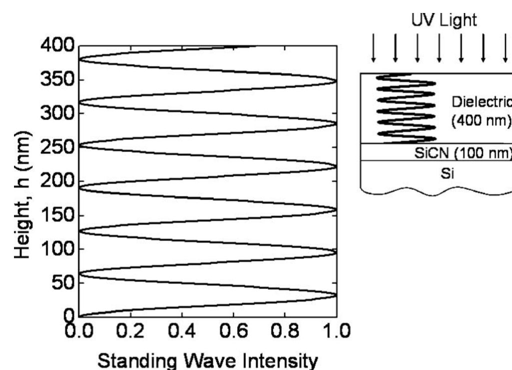

FIG. 10. The standing wave intensity envelope of the UV light in the as-deposited 400 nm thick organosilicate film. The intensity was normalized by the amplitude of the standing-wave I_0.

sible that only small variations of composition below the limit of resolution of our characterization would be needed to explain the stiffness variations observed; in light of the mechanism described below, we believe that while some contribution from spinodal decomposition cannot be ruled out, it is likely not the dominant process in forming the stiffness variations observed.

Although not initially anticipated, another possible mechanism may be related to depth dependent UV curing associated with the formation of UV standing wave effects. Such standing waves caused by UV light interference are well known in optical lithography. They lead to variations in the light intensity perpendicular to the resist film producing an undesirable side effect of the exposure process.[30–32,34] When a thin dielectric film placed between two semi-infinite media (e.g., the thin organosilicate film on a reflecting silicon substrate) is exposed to monochromatic light, standing waves are produced in the film.[33] Neglecting the effect of resist absorption, the intensity envelope of resulting standing waves that occur in a thin film on a perfectly reflecting substrate is given by[34]

$$I = I_0 \sin^2 k(d - z), \tag{1}$$

where I_0 is the amplitude of the standing wave which is film thickness dependent, $k=2\pi n/\lambda$ (n is the real part of the film index of refraction and λ is the wavelength of the incident light), d is the thickness of the film, and z is the depth into the thin film. It is important to note that in the case of polychromatic exposure, for example, UV spectra with distinct peaks, the resulting standing wave is the result of the superposition of each individual peak wavelength given by Eq. (1).[34] The UV standing wave intensity envelope for the monochromatic light used in the present study with wavelength <200 nm through the thickness of the organosilicate film is plotted in Fig. 9 using Eq. (1). A refractive index of 1.36 was employed for the organosilicate glass and the existence of absorption in the SiCN bottom layer was neglected for simplicity. During UV curing of the organosilicate film, the photochemical curing reaction would occur to greater extent at regions of higher light intensity leading to a periodic variation of curing through the thickness of the film. In fact, the wavelength of the standing wave apparent in Fig. 10 is similar to that observed for the FM-AFM stiffness variation shown in Fig. 3. In addition, the magnitude of the stiffness variation increased with increasing cure time as shown in Fig. 4. A more complete model to account for the effect of film shrinkage and changing refractive index during cure together with UV light absorption and reflection at the film interfaces is the subject of our ongoing research and is presented elsewhere.[35]

We now describe how the UV standing wave effect may be used to rationalize the resulting fracture energy dependence on organosilicate film thickness and how it may contribute to the insensitivity of the cohesive fracture energy following UV curing. As can be easily deduced from Fig. 10, the intensity of the UV standing wave at the top of the organosilicate film will vary with the thickness of the film, while the intensity at the bottom perfectly reflecting interface will be zero regardless of the thickness. This will result in different amounts of curing at the top of the layer depending on the exact thickness of the film and the resulting intensity of the standing wave at that location. However, more importantly, the film shrinks significantly during cure, meaning that the intensity will vary as the top of the film passes through minima and maxima of the standing wave leading to some averaging of the cure intensity. In addition, UV absorption occurs through the film thickness leading to reduced standing wave intensity with increasing film thickness. We present a detailed model for this phenomenon elsewhere.[35] The net effect is to significantly increase the cure towards the top of the film, particularly when the film is thinner. The thickness dependent variation of the resulting fracture energy measured at the top of the layer sensitively reflects this variation of the local UV cure [Fig. 6(a)]. However, we caution that the exact extent of curing is sensitive to the exact initial film thickness. Small variations of the initial thickness can lead to significantly different curing at the top of the layer within an envelope of maxima and minima of the resulting standing wave. This effect is reflected in the apparently constant fracture energy for the initially 600 and 800 nm films as shown in Fig. 6(a).

Downloaded 21 Apr 2013 to 143.248.118.125. This article is copyrighted as indicated in the abstract. Reuse of AIP content is subject to the terms at: http://jap.aip.org/about/rights_and_permissions

The resulting standing wave forms an essentially zero intensity node at the bottom reflecting interface of the organosilicate film with the silicon substrate. Partial absorption by the silicon substrate can occur and is considered elsewhere.[35] However, the main point is that significantly less curing is expected over distances from the bottom interface corresponding to ~ 1/8 of the standing wave wavelength, which for the present study corresponds to ~10 nm. This is the same region in which the bottom fracture energy was measured. Careful calculations of the standing wave in this region reveal that increased UV cure intensity occurs for thinner films,[35] and this results in the marginal increase in fracture energy reported for the bottom interface with decreasing film thickness (Fig. 6). We note finally that through the depth of the film, multiple locations exist that represent minima of the UV standing wave and hence regions of minimum UV cure. We therefore expect that cohesive fracture energy measurements represent fracture along these planes of reduced curing and hence glass network connectivity (Figs. 7 and 8). The crack essentially finds the weakest fracture path in the glass network as previously reported,[10,12] but in this case, aided by planes of lower curing.

The study clearly reveals the importance of UV standing waves that may form during UV cure, and immediately suggests the possibility of modifying the nature and wavelength of the standing wave by changing the reflectivity of the underlying barrier or etch stop layer. For example, the UV absorption and reflectivity of an underlying amorphous SiCN thin layer could be adjusted by varying the carbon content of the film.[36,37] This would have significant effects on the resulting standing wave and even the position of the standing wave minima at the bottom interface with the SiCN film. Preliminary results suggest that the fracture energy at the bottom interface can be increased by ~25% with a SiCN under layer, compared to only ~14% without the layer. Such interface engineering represents an important strategy that may be exploited to locally cure towards the bottom interface, even in the presence of broadband UV curing, and is the subject of our ongoing research. In addition, this approach also suggests the possibility of creating a desired cure profile through the film thickness by careful control of the resulting standing wave intensity.

CONCLUSIONS

This study presents the evidence of depth dependence of UV curing of organosilicate low-*k* thin films, which has important effects on through thickness mechanical and fracture properties. Oscillations of the elastic modulus through the UV cured films were observed using FM-AFM measurements. The amplitude of the oscillation increased with extended UV curing. Significant increases in fracture energy were observed with UV curing time at the top of the organosilicate film while much lower increases were observed at the bottom of the layer. The increase in fracture energy with UV curing was film thickness dependent. The cohesive fracture resistance was less sensitive to UV curing. Possible explanations for the depth dependent UV curing are presented and include phase separation by spinodal decomposition and standing wave effects resulting from UV light interference through the film thickness. Depth dependent UV curing was employed to rationalize the fracture energy variation measured in different locations of the film depth, and the effects of changing film thickness.

ACKNOWLEDGMENTS

The authors acknowledge assistance with sample preparation by Yvonne Ritz of AMD in Dresden. This work was supported by the Director, Office of Energy Research, Office of Basic Energy Sciences, Materials Sciences Division of the U.S. Department of Energy, under Contract No. DE-FG02-07ER46391. One of the authors (T.S.K.) was supported in part by ASM Japan K.K.

[1] E. P. Guyer and R. H. Dauskardt, Nat. Mater. **3**, 53 (2004).
[2] E. P. Guyer and R. H. Dauskardt, Proceedings of the 2003 IEEE International Interconnect Technology Conference, 2003.
[3] E. P. Guyer and R. H. Dauskardt, "Accelerated Crack Growth of Nanoporous Low-*k* Glasses in CMP Slurry Environments," Proceedings of the 2004 IEEE International Interconnect Technology Conference, 2004.
[4] E. P. Guyer and R. H. Dauskardt, "Effects of Porosity on Reducing Cohesive Strength and Accelerating Crack Growth in Ultra Low-*k* Thin-Films," Proceedings of the 2005 IEEE International Interconnect Technology Conference, 2005.
[5] H. Namatsu and K. Minegishi, J. Electrochem. Soc. **140**, 1121 (1993).
[6] G. Kloster, T. Scherban, G. Xu, J. Blaine, B. Sun, and Y. Zhou, "Porosity Effects on Low-*k* Dielectric Film Strength and Interfacial Adhesion," Proceedings of the 2002 IEEE International Interconnect Technology Conference, 2002 (unpublished).
[7] J. J. Y. Ma, S. F. C. Tseng, K. W. T. Chien, and V. W. W. Ruan, "Stress Migration Related Reliability Concerns," Proceedings of the 43rd Annual IEEE International Reliability Physics Symposium, 2005.
[8] F. Iacopi, Y. Travaly, B. Eyckens, C. Waldfried, T. Abell, E. P. Guyer, D. M. Gage, R. H. Dauskardt, T. Sajavaara, K. Houthoofd, P. Grobet, P. Jacobs, and K. Maex, J. Appl. Phys. **99**, 053511 (2006).
[9] F. Iacopi, G. Beyer, Y. Travaly, C. Waldfried, D. M. Gage, R. H. Dauskardt, K. Houthoofd, P. Jacobs, P. Adriaensens, K. Schulze, S. E. Schulz, S. List, and G. Carlotti, Acta Mater. **55**, 1407 (2007).
[10] D. M. Gage, J. F. Stebbins, L. Peng, Z. Cui, A. Al-Bayati, K. P. MacWilliams, H. M'Saad, and R. H. Dauskardt, "Effects of UV Cure on Glass Structure and Fracture Properties of Nanoporous Carbon-Doped Oxide Thin Films," J. Appl. Phys. (submitted).
[11] H. Okabe, *Photochemistry of Small Molecules* (Wiley, New York, 1978).
[12] D. M. Gage, E. P. Guyer, J. F. Stebbins, Z. Cui, A. Al-Bayati, A. Demos, K. P. MacWilliams, and R. H. Dauskardt, "UV Curing Effects on Glass Structure and Mechanical Properties of Organosilicate Low-*k* Thin Films," Proceedings of the 2006 IEEE International Interconnect Technology Conference, 2006.
[13] K. Yoneda, M. Kato, S. Kondo, N. Kobayashi, N. Matsuki, K. Matsushita, N. Ohara, A. Fukazawa, and T. Kimura, "Impacts of UV Cure for Reliable Porous PECVD SiOC Integration," Proceedings of the 2005 IEEE International Interconnect Technology Conference, 2005.
[14] T. Kim, N. Tsuji, N. Kemeling, K. Matsushita, and R. H. Dauskardt, "Non-Uniform UV Curing Effects on Mechanical and Fracture Properties of Organosilicate Low-*k* Thin Films," Proceedings of Advanced Metallization Conference 2006.
[15] L. Landau and E. Lifshitz, *Teoriya Uprugosti* (Nauka, Moscow, 1987), pp. 44–50.
[16] D. Chumakov, H. Geisler, L. Jiang, and E. Zschech, AIP Conf. Proc. **817**, 110 (2006).
[17] E. Zschech, H. Stegmann, P. Hoffmann, D. Schmeisser, P. Potapov, H. J. Elgelmann, D. Chumakov, and H. Geisler, Mater. Res. Soc. Symp. Proc. **914**, F11 (2006).
[18] R. J. Hohlfelder, D. A. Maidenberg, R. H. Dauskardt, Y. Wei, and J. W. Hutchinson, J. Mater. Res. **16**, 243 (2001).
[19] R. H. Dauskardt, M. Lane, Q. Ma, and N. Krishna, Eng. Fract. Mech. **61**, 141 (1998).
[20] M. F. Kanninen, Int. J. Fract. **9**, 83 (1973).
[21] E. P. Guyer and R. H. Dauskardt, J. Mater. Res. **19**, 3139 (2004).

Downloaded 21 Apr 2013 to 143.248.118.125. This article is copyrighted as indicated in the abstract. Reuse of AIP content is subject to the terms at: http://jap.aip.org/about/rights_and_permissions

[22]T. Kim, D. Chumakov, Y. Ritz, H. Geisler, E. Zschech, and R. H. Dauskardt (unpublished).
[23]M. Tomozawa, J. Am. Ceram. Soc. **61**, 444 (1978).
[24]S. Y. Park, R. A. Weeks, and R. A. Zuhr, "Laser Induced Diffusion of Ion-Implanted Bismuth in Fused Silica," Proceedings of the Fifth International 5th Inter. Otto Schott Colloquium, 1994 (unpublished).
[25]F. Kherbouche, B. Poumellec, F. Charpentier, and P. Niay, J. Phys. D **33**, 3233 (2000).
[26]J. W. Cahn, Trans. Soc. Min. Eng. AIME **242**, 166 (1968).
[27]J. W. Cahn and R. J. Charles, Phys. Chem. Glasses **6**, 181 (1965).
[28]J. W. Cahn and J. E. Hilliard, J. Chem. Phys. **28**, 258 (1958).
[29]G. Krausch, C. Dai, E. J. Kramer, and J. F. Markotpo, Macromolecules **26**, 5566 (1993).
[30]L. F. Thompson, C. G. Willson, and M. J. Bowden, *Introduction to Microlithography* (American Chemical Society, Washington, DC, 1994), pp. 81–85.
[31]F. H. Dill, IEEE Trans. Electron Devices **22**, 440 (1975).
[32]F. H. Dill, A. R. Neureuther, J. A. Tuttle, and E. J. Walker, IEEE Trans. Electron Devices **22**, 456 (1975).
[33]C. A. Mack, Appl. Opt. **25**, 1958 (1986).
[34]J. D. Cuthbert, Solid State Technol. **50**, 59 (1977).
[35]T. Kim, N. Tsuji, K. Matsushita, N. Kobayashi, D. Chumakov, H. Geisler, E. Zschech, and R. H. Dauskardt (unpublished).
[36]C. W. Chen, C. C. Haung, Y. Y. Lin, L. C. Chen, K. H. Chen, and W. F. Su, Diamond Relat. Mater. **14**, 1010 (2005).
[37]C. W. Chen, C. C. Haung, Y. Y. Lin, W. F. Su, L. C. Chen, and K. H. Chen, Appl. Phys. Lett. **88**, 073515 (2006).

Downloaded 21 Apr 2013 to 143.248.118.125. This article is copyrighted as indicated in the abstract. Reuse of AIP content is subject to the terms at: http://jap.aip.org/about/rights_and_permissions